

# Iris Recognition: Feature Extraction and Comparison from Noisy Images

Hugo Proença and Luís A. Alexandre

Dep. Informatics, Universidade da Beira Interior  
IT - Networks and Multimedia Group, Covilhã  
R. Marquês D'Ávila e Bolama, 6200-001, Covilhã, Portugal  
{hugomcp, lfbaa}@di.ubi.pt

**Abstract.** Iris recognition is being increasingly used for several purposes. However, current iris recognition systems are unable to deal with noisy data and substantially increase their error rates, specially the false rejections in these conditions. Several proposals have been made to assess image quality and to identify noisy regions in iris images. Based in these facts, in this paper we propose a method applicable in the feature extraction and comparison stages that measures the quality of each feature of the biometric signature and take account of this information to obtain the dissimilarity between iris signatures. Experiments led us to conclude that this method significantly decreases the error rates in the recognition of noisy iris images, resultant from the capturing in less constrained environments.

**Keywords:** feature quality, feature extraction, feature comparison, non-cooperative iris recognition, biometrics.

## 1 Introduction

Since 1987, when L. Flom and A. Safir [6] concluded about the stability of iris morphology and estimated the probability for the existence of two similar irises at 1 in  $10^{72}$ , the use of iris based biometric systems has been increasingly encouraged by both government and private entities. Iris is commonly recognized as one of the most reliable biometric measures: it has a random morphogenesis and no genetic penetrance.

Iris recognition is presently used for several purposes with very satisfactory results. Under rigid image capture conditions it is possible to obtain good quality images and achieve impressive accuracy, with very low error rates. However, these error rates substantially increase, specially the false rejections, when the images do not have enough quality, either due to focus, contrast or brightness problems, iris obstructions or reflections. This is a problem commonly identified by several authors (e.g. [23], [15] and [22]).

From our viewpoint, the challenge for iris recognition consists in the ability to achieve accurate identification in less constrained image capture environments, either under natural luminosity or heterogeneous lighting conditions.

These conditions lead to the appearance of very heterogeneous images and with several noise factors, namely poor focused and with iris reflections or obstructions, as exemplified by figure 1. Thus, the robustness of iris recognition algorithms and their ability for noise identification and handling becomes indispensable to achieve accurate recognition in less constrained environments.

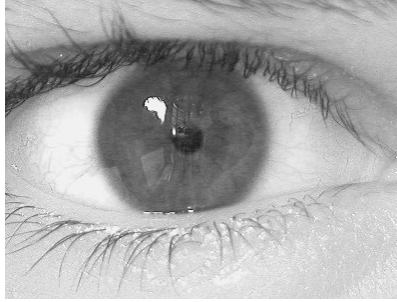


**Fig. 1.** Noisy iris image with eyelid and eyelash obstructions and a large reflection area

In this paper we propose a method for measuring the quality of each feature extracted from the iris, since there is a significant increment of the error rates of typical iris recognition systems when images are highly heterogeneous or contain significant portions of noise [10]. This measure is based in the proportion of noisy pixels used in the extraction of the feature and will be further used in the feature comparison stage, in order to achieve robustness to noisy images.

As we describe in the next sections, we used images from the UBIRIS [18] database, highly heterogeneous and with noisy characteristics, to compare the results obtained by the classical Daugman recognition method as described by the author [4] and together with our quality measure and comparison proposals.

The remainder of this paper is organized as follows: section 2 briefly summarizes the most cited iris recognition methods emphasizing the features extraction and comparison stages. A detailed description of the proposed method is given in section 3. Section 4 reports the experiments and results and finally section 5 concludes this paper.

## 2 Iris Recognition Systems

In spite of the distinct approaches proposed by different authors for each stage, typical iris recognition systems share a common structure that is illustrated on figure 2.

The initial stage deals with iris segmentation. This process consists in, approximating the iris as a circumference or an ellipse, localize the iris inner (pupillary) and outer (scleric) borders. There are two major strategies for iris segmentation: using a rigid or deformable template of the iris or its boundary. In most cases, the boundary approach is very similar to the proposed by Wildes [23]: it begins by the construction of an edges

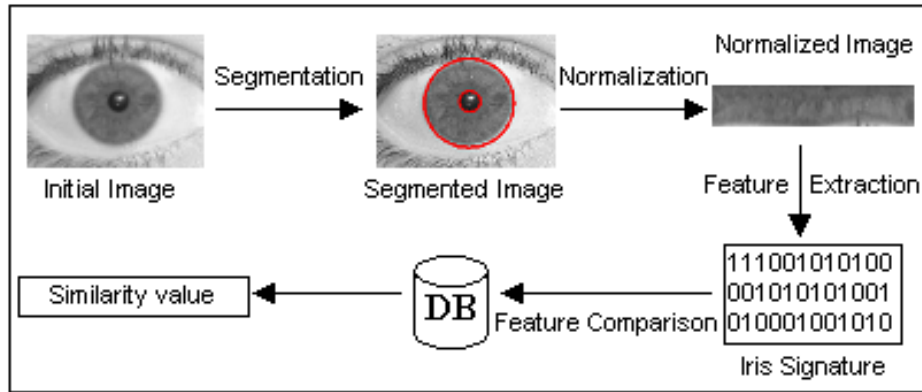


Fig. 2. Typical stages of the iris recognition systems

map followed by the application of some geometric form fitting algorithm. Authors of [19] used this strategy together with a clustering process to increase accuracy in noisy environments. The template-based strategies usually involve the maximization of some equation, as proposed by Daugman [4] and Roche et. all [16].

In order to compensate the varying size of the pupil it is common to translate the segmented iris part represented in the cartesian coordinate system to a fixed length and dimensionless polar coordinate system. This is usually accomplished through a method similar to the Daugman's Rubber Sheet [4].

The next stage is the feature extraction. From this viewpoint, iris recognition approaches can be divided in three major categories: phase-based methods (e.g. [4]), zero crossing methods (e.g. [2] and [16]) and texture analysis based methods (e.g [23], [11] and [14]).

Having a feature set, commonly named biometric iris signature, the final stage consists in the comparison between signatures, producing a numeric dissimilarity value. If this value is higher than a threshold, the system outputs a "non-match", meaning that each signature belongs to different subjects. Otherwise, the system outputs a "match", meaning that both signatures were extracted from the same person.

## 2.1 Feature Extraction and Comparison Methods

In the feature extraction stage, Daugman [4] uses multiscale quadrature wavelets to extract texture phase information and obtain an iris signature with 2048 binary components. To characterize the texture from the iris, Boles and Boashash [2] computed the zero-crossing representation of a 1D wavelet at different resolutions of concentric circles. Wildes [23] proposes the characterization of the iris texture through a Laplacian pyramid with 4 different levels (scales). This pyramid is further used to compute the normalized correlation between images and conclude about their similarity.

One of the most typical approaches constitutes the proposal of [12], characterizing the iris texture through its decomposition by the dyadic wavelet transform, either us-

ing Haar, Daubechies or other mother wavelets. This approach was found with minor variants in several other works (e.g. [20], [1]).

Regarding the feature comparison stage, it is constrained by the feature extraction method. When the produced iris signature is binary, it is common to apply the Hamming distance metric. Otherwise, different metrics like the Euclidean (e.g. [8]), Weighted Euclidean (e.g. [24], [14]) or methods based on signal correlation (e.g [23]) can be applied. More specific approaches were proposed by Lim et. al [12] through the use of a competitive learning neural network to achieve classification and Ma et. al [13] that use a modified nearest neighbor to compare the acquired and the enrolled samples and assign the proper entity.

## 2.2 Noise Identification

The problem of noise identification in iris images has been recently addressed by several authors, constituting one of the most challenging domains in the present iris recognition research.

Daugman [4] builds a binary noise mask for iris image to identify eyelids and eyelashes that obstruct iris and can deteriorate results.

The authors of [3] were based in the analysis of the energy resultant from the convolution between the image and a group of Mexican-Hat Wavelets at 3 different scales to propose local and global iris image quality measures.

The purpose of [7] was the identification of four distinct types of noise: eyelashes, eyelids, reflections and pupil. The idea is that there's always some type of edges between the noisy and the noise-free areas. Those edges were identified through an illumination invariant measure (phase congruency).

The later methods operate locally and produce a binary map where each pixel is classified as "noisy" or "noise-free". Our feature quality measure and further comparison strategy is based in this binary map. Starting from it, we obtain a confidence (quality) value for each feature based in the noise classification from the pixels that were used in its creation. Furthermore, we use this quality value in the feature comparison stage to select the comparable features and improve the ability of the iris recognition system to handle noisy images.

## 3 Proposed Feature Quality Measure and Comparison Methods

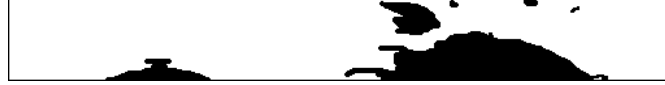
As referred above, the local noise identification methods described in section 2.2 produce a binary map correspondent to the segmented and normalized iris image. In this map the noisy regions correspond to the dark areas whereas the noise-free regions are represented through white areas (figure 3).

For each of the extracted features from the image we create a quality value contained in the  $[0,1]$  interval that reflects the proportion of noisy pixels used in the respective calculus. This value will be helpful in the feature comparison stage, avoiding the utilization of the noisiest features or assigning them a small weight for the comparison.

As described in the next section, the proposed feature quality measure is independent from the feature extraction method. At a coarse level, every extracted feature can



(a) Segmented and normalized iris image with large noisy regions correspondent to eyelids (1) and eyelashes (2) obstructions and reflections (3).



(b) Identification of the noisy regions from the image 3a.

**Fig. 3.** Identification of the noisy regions in a normalized iris image.

be regarded as function of  $K$  pixels from the image (the original data). Thus, the calculus of the proportion of noisy and noise-free pixels used in its extraction can be applied to any methodology.

### 3.1 Feature Quality Measure

Let  $I$  be the segmented and normalized iris image and  $(x, y) \in \mathbb{N}^2$  be the coordinates of a pixel from the image. Let  $n((x, y)) : \mathbb{N}^2 \rightarrow \{0, 1\}$  be the function that classifies as "noisy" or "noise-free" every pixel  $(x, y)$  from the image  $I$ :

$$n((x, y)) = \begin{cases} 1, & \text{I(x,y) is noisy} \\ 0, & \text{otherwise} \end{cases} \quad (1)$$

Let  $\mathbb{F} = \{f_1, \dots, f_k\}$  be the set of features extracted from the image  $I$ . At the coarsest level, every  $f_i$  arises from the calculus between  $N_i$  pixels from  $I$ . Let  $\mathbb{P}_i = \{(x_{i_j}, y_{i_j})\} j = 0, \dots, N_i - 1$  be the set of coordinates from the pixels used in the extraction of the feature  $f_i$ . We define the function  $c(\mathbb{P}_i) : (\mathbb{N}_0^2 \times \dots \times \mathbb{N}_{N-1}^2) \rightarrow [0, 1]$  that gives the quality of the feature  $f_i$ :

$$c(\mathbb{P}_i) = \frac{1}{N_i} \sum_{i=0}^{N_i} n(I(x_i, y_i)) \quad (2)$$

where  $N_i$  is the cardinality of  $\mathbb{P}_i$ .

Through this method, for every extracted feature we obtain a quality value contained in the  $[0,1]$  interval. This value has inverse correspondence with the proportion of noisy pixels that were considered in the creation of  $f_i$ . Thus, for completely "noisy" (poorest quality) and "noise-free" (optimal quality) features the quality value will be, respectively, equal to 0 and 1.

### 3.2 Feature Comparison

In the following discussion we will use a superscript to distinguish between two different feature sets, such as,  $f^1$  and  $f^2$ , and a subscript to distinguish between different features from a feature set, such as,  $f_1^1$  and  $f_2^1$ .

In the feature comparison stage it is obtained a similarity value that reflects the respective similarity between two feature sets  $\mathbb{F}^i$  and  $\mathbb{F}^j$  and enables the assumption about the identity of the subjects from which the features were extracted. In this section, we describe the two tested variants for the feature comparison: "hard" and "fuzzy".

In the "hard" feature comparison, features are considered for comparison only if their quality value is higher than a threshold. Oppositely, in the "fuzzy" feature comparison variant the comparison is allowed for any feature, independently of its quality value. The result is weighted with the average quality value from the feature operands.

Formally, let  $Q^0$  and  $Q^1$  be two features sets with the respective quality value for each feature,  $Q^j = \{(f_1^j, c(f_1^j)), \dots, (f_n^j, c(f_n^j))\}$ . The feature comparison function is given by:

$$fc(Q^0, Q^1) = \sum_{i=1}^n \frac{dist(f_i^0, f_i^1)}{cnt(f_i^0, f_i^1)} \quad (3)$$

In the "hard" comparison variant,  $dist$  and  $cnt$  are functions given by:

$$dist_{hard}(f_i^0, f_i^1) = \begin{cases} d(f_i^0, f_i^1), & c(f_i^0) \geq T, c(f_i^1) \geq T \\ 0, & \text{otherwise} \end{cases} \quad (4)$$

$$cnt_{hard}(f_i^0, f_i^1) = \begin{cases} 1, & C(f_i^0) \geq T, C(f_i^1) \geq T \\ 0, & \text{otherwise} \end{cases} \quad (5)$$

where  $d$  is the function that gives the distance between features (e.g. Hamming, Euclidean distance, ...).

In the "fuzzy" comparison variant, all the features are considered for comparison and weighted regarding their quality value. Thus,  $dist$  and  $cnt$  are given by:

$$dist_{fuzzy}(f_i^0, f_i^1) = d(f_i^0, f_i^1) * \frac{c(f_i^0) + c(f_i^1)}{2} \quad (6)$$

$$cnt_{fuzzy}(f_i^0, f_i^1) = \frac{c(f_i^0) + c(f_i^1)}{2} \quad (7)$$

where, as above,  $d$  is the function that gives the distance between features.

## 4 Experiments and Discussion

We implemented the method described by Daugman [4]. We compared the obtained results when following the method as described by the author (using all the features in the feature comparison stage) and our proposal feature confidence measure and feature comparison methods.

As described in [4], the Daugman's recognition method is composed by the following stages:

- Iris segmentation. We implemented the integrodifferential operator proposed by the author to find both the inner and outer iris borders, given by:

$$\max_{r, x_0, y_0} \left| G_\sigma(r) * \frac{\delta}{\delta r} \oint_{r, x_0, y_0} \frac{I(x, y)}{2\pi r} ds \right|$$

This operator searches over the image domain  $(x, y)$  for the maximum in the blurred partial derivative with respect to increasing radius  $r$ , of the normalized contour integral of  $I(x, y)$  along a circular arc  $ds$  of radius  $r$  and center coordinates  $(x_0, y_0)$ .

- Normalization. To compensate the variations in the size of the pupil, we translated the images to dimensionless polar coordinate system through a process known as the "Daugman Rubber Sheet" [4]. The remapping of the iris image  $I(x, y)$  to the polar coordinate system  $I(r, \theta)$  can be represented as:

$$I(x(r, \theta), y(r, \theta)) \rightarrow I(r, \theta)$$

with  $x(r, \theta) = (1-r)x_p(\theta) + rx_i(\theta)$  and  $y = (1-r)y_p(\theta) + ry_i(\theta)$ , where  $(x_p, y_p)$  and  $(x_i, y_i)$  are the coordinates of the identified inner and outer iris boundaries along the angular  $(\theta)$  direction.

- Feature Extraction. The iris data encoding was accomplished through the use of two dimensional Gabor filters. These spatial filters have the form:

$$G(x, y) = e^{-\pi[(x-x_0)^2/\alpha^2 + (y-y_0)^2/\beta^2]} \cdot e^{-2\pi i[u_0(x-x_0) + v_0(y-y_0)]}$$

where  $(x_0, y_0)$  defines the position in the image,  $(\alpha, \beta)$  is the filter width and length and  $(u_0, v_0)$  specify the modulation, having spatial frequency  $w_0 = \sqrt{u_0^2 + v_0^2}$  and direction  $\theta_0 = \arctan(v_0/u_0)$ .

The real parts of the 2-D Gabor filters are truncated to be zero volume and achieve illumination invariance. For each resulting bit we analyzed the sign of the real and imaginary parts from quadrature image projections and through quantization assigned binary values: 1 and 0 respectively for positive and negative projection values.

- Feature Comparison. The feature extraction binarization process allows the utilization of the Hamming distance as the similarity measure for two iris signatures. Given two binary sets with  $N$  bits:  $A = \{a_1, \dots, a_N\}$  and  $B = \{b_1, \dots, b_N\}$ , the Hamming distance is:

$$HD(A, B) = \frac{1}{N} * \sum_{i=1}^N a_i \otimes b_i$$

being  $a \otimes b$  the logical "XOR" operation. Thus, for two completely equal and different signatures, the value of the Hamming distance will be respectively 0 and 1.

The identification of the noisy pixels in the normalized iris image was accomplished following the method described in [3]. This method produces a binary map with the noisy pixels correspondent to the dark regions, as exemplified by figure 3b.

Through the process described in section 3 we obtain a quality measure for each feature of the biometric signature. Hereinafter, the task consists in determining the features that must be compared in order to maximize the separability between the intra and inter-class comparisons (respectively resultant from images from the same and different irises).

In the limit, if all the features are compared, the probability that some of these features are corrupted by noise and deteriorate the results is maximized. Oppositely, if the feature comparison is exclusively made between features with optimal quality value (completely noise-free), the number of comparisons is minimized, propitiating that random similarities or dissimilarities between iris signatures also deteriorate the final similarity value between signatures.

Thus, the number of comparable features must deny the comparison between extremely low-confidence features while maintaining a sufficient large number of comparisons, in order to avoid that random (dis) similarities between features can significantly change the final result.

In the experiments, we varied both the feature comparison variant and the minimum quality value demanded for comparable features and analyzed the recognition accuracy in two distinct data sets with different noise quantities. In the next section we present the available data sets and justify our choice.

#### 4.1 Data Sets

There are presently 5 public and free available iris image databases for biometric purposes: CASIA [9], MMU [17], BATH [21], UPOL [5] and UBIRIS [18].

CASIA database is by far the most widely used for biometric purposes. However, its images incorporate few types of noise, almost exclusively related with eyelid and eyelash obstruction. MMU and BATH databases contain very homogeneous images, and with few noise factors. UPOL images were captured with an optometric framework, resulting in optimal images with extremely similar characteristics. Oppositely, UBIRIS database was builded with the objective of simulating non-cooperative capturing. This facts explains the higher heterogeneity of its images and the existence of several types of noise: eyelid and eyelashes obstruction, poor focused and with different types of reflections (light sources next to the users and information from the environment that surrounds them). These facts make it the most appropriate for the objectives of our work and led us to choose UBIRIS as the main database for our experiments.

We initially selected 260 images from the UBIRIS database, belonging to 26 different subjects (10 images from each subject). Figure 4 contains examples from the images used in our experiments. However, we considered relevant to obtain information about the recognition accuracy as the amount of noise in the image varies. To enable this analysis, we further divided the selected images in two sub sets, according to their noise characteristics. The 130 less noisy images were included in the  $UBIRIS_F$  data set and the 130 noisier ones in the  $UBIRIS_N$  data set.

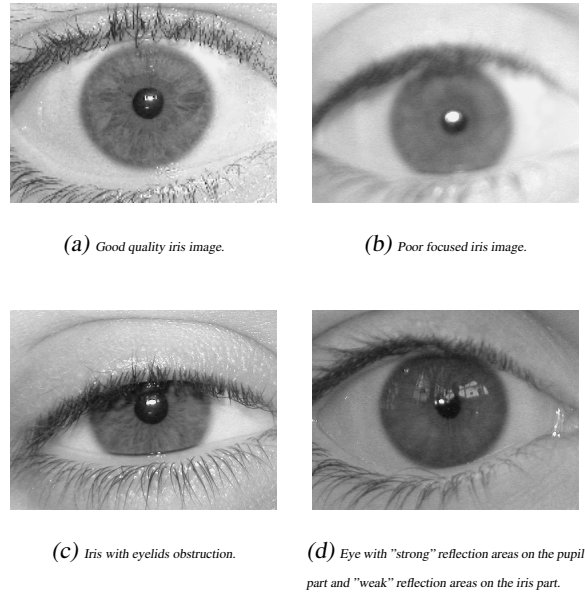


**Fig. 4.** Examples of images from the UBIRIS database.

## 4.2 Results

According to the process described in section 4, we compared the accuracy of the classical Daugman methodology as described by the author and together with our proposals in the above described data sets ( $UBIRIS_F$  and  $UBIRIS_N$ ).

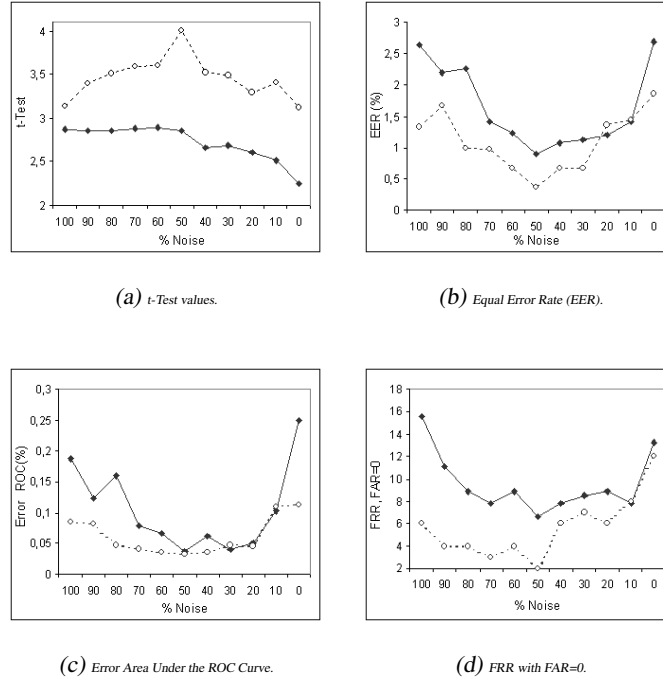
Figure 5 contains 4 measures that reflect the advantages of applying our proposal together with the classical Daugman feature extraction and comparison methodologies. The horizontal axis represents the minimum feature quality value using the "hard" comparison variant. The traditional approach of comparing all the features is equivalent to our proposal with minimum quality value equal to 0. The continuous line is relative to the  $UBIRIS_N$  data set and the dashed line to the less noisier  $UBIRIS_F$  data set.

Figure 5a contains the obtained values for a t-test given by:

$$\tau = \frac{\mu^E - \mu^I}{\sqrt{\frac{\sigma^I{}^2}{N^I} + \frac{\sigma^E{}^2}{N^E}}} \quad (8)$$

where symbols  $\mu^I$  and  $\mu^E$  respectively indicate the obtained means in the intra-class (images from the same iris) and inter-class (images from different irises) comparisons.  $\sigma^I$  and  $\sigma^E$  indicated the respective standard deviations and  $N^I$  and  $N^E$  are, respectively, the total number of intra-class and inter-class comparisons between iris signature.

Figure 5b contains the equal error rates, obtained when the false accepts and rejects are approximately equal. Figure 5c contains the percent values for the area under the



**Fig. 5.** Obtained results from our proposal in the  $UBIRIS_N$  (continuous line) and  $UBIRIS_F$  (dashed line).

receiver operating curve (ROC) and figure 5d contains the obtained value for the false rejections, when the false acceptances are minimized.

The best results were obtained when the feature comparison was enabled between features with minimum quality value around 0.5 (50%). In this situation, while maintaining a large number of comparable features, it is avoided that very poor quality features, extracted from large proportion of noisy pixels, corrupt the final results.

Our experiments clearly show an improvement of the system's accuracy, significantly reducing the error rates, the area under the ROC and increasing the separability between the intra-class inter-class comparisons.

Table 1 contains the obtained results, when varying the feature comparison strategy. The first column identifies the classification method. The second ( $\tau$ ) contains the value for the t-test described above, the third column the equal error rate and the last column the obtained false rejection rate when the false acceptances were minimized. All the error values are expressed for a confidence interval of 95%.

The analysis of these results clearly shows an increment of system's overall accuracy using our proposal - with the "hard" variant, specially in the noisier  $UBIRIS_N$  data set. In the less-noisier  $UBIRIS_F$  data set the results were more similar, mean-

| Method                             | $\tau$ | EER (%)        | Error ROC (%) | FRR, FAR=0 (%)  |
|------------------------------------|--------|----------------|---------------|-----------------|
| <i>UBIRIS<sub>N</sub></i> data set |        |                |               |                 |
| Original                           | 2.258  | 2.090 ± 0.0040 | 0.449         | 15.556 ± 0.0101 |
| Proposed (Hard), T=0.5             | 2.892  | 0.904 ± 0.0026 | 0.036         | 6.667 ± 0.0070  |
| Proposed (Fuzzy)                   | 2.699  | 1.130 ± 0.0029 | 0.057         | 11.639 ± 0.0090 |
| <i>UBIRIS<sub>F</sub></i> data set |        |                |               |                 |
| Original                           | 3.130  | 2.690 ± 0.0045 | 0.112         | 12.778 ± 0.0093 |
| Proposed (Hard), T=0.5             | 4.012  | 0.366 ± 0.0016 | 0.032         | 2.667 ± 0.0045  |
| Proposed (Fuzzy)                   | 3.813  | 0.900 ± 0.0026 | 0.058         | 6.166 ± 0.0067  |

**Table 1.** Obtained Results.

ing that even in images with insignificant portions of noise our proposal can slightly improve the recognition's accuracy.

With the "fuzzy" feature comparison variant, we obtained worst results than with the "hard" one. The comparison of all the features, even if they are weighted with their quality value, is not a valid alternative.

## 5 Conclusions

In this paper we proposed a method for the measurement of the quality of each extracted feature for iris recognition systems. The motivation for this work was the significant increment of the error rates when these systems deal with noisy images.

The quality is used to constraint the number of components that are taken into account in the feature comparison stage. Experiments led us to conclude that this method significantly decreases the error rates in the recognition of noisy iris images, thus being appropriate for the application in a non-cooperative recognition compass, where the ability to deal with noisy images is required.

Even in images with better quality, with minor portions of noise, the results showed that our quality measure contributes for the selection of the best features with the correspondent achievement in the recognition system's accuracy.

Moreover, the fact that our proposal is independent of the chosen feature extraction and comparison methodology can be regarded as a strong point. The analysis of the benefits of its application in other iris recognition strategies (feature extraction and feature comparison) is one direction for the future work.

## References

1. Jafar Ali and Aboul Hassani. An iris recognition system to enhance e-security environment based on wavelet theory. *AMO - Advanced Modeling and Optimization*, vol. 6, no. 2, pages 93–104, 2003.
2. W. W. Boles and B. Boashash. A human identification technique using images of the iris and wavelet transform. *IEEE Transactions on Signal Processing*, vol. 46, no. 4, pages 1185–1188, April 1998.

3. Yi Chen, Sarat C. Dass, and Anil K. Jain. Localized iris image quality using 2-D wavelets. In *Proceedings of the 2006 International Conference on Biometric*, pages 373–381, Hong Kong, 2006.
4. John G. Daugman. High confidence visual recognition of persons by a test of statistical independence. *IEEE Transactions on Pattern Analysis and Machine Intelligence*, vol. 15, no. 11, pages 1148–1161, November 1993.
5. Michal Dobes and Libor Machala. UPOL iris image database, 2004. <http://phoenix.inf.upol.cz/iris/>
6. L. Flom and A. Safir. Iris recognition system, 1987. U.S. Patent 4 641 394.
7. Junzhou Huang, Yunhong Wang, Tieniu Tan, and Jiali Cui. A new iris segmentation method for recognition. In *Proceedings of the 17th International Conference on Pattern Recognition (ICPR04)*, vol. 3, pages 23–26, 2004.
8. Ya Huang, Si Luo, and En Chen. An efficient iris recognition system. In *Proceedings of the First International Conference on Machine Learning and Cybernetics*, pages 450–454, China, November 2002.
9. Institute of Automation, Chinese Academy of Sciences. CASIA iris image database, 2004. <http://www.sinobiometrics.com>
10. International Biometric Group. Independent test of iris recognition technology, 2005. <http://www.biometricgroup.com/reports/public/ITIRT.html>
11. Jaemin Kim, Seongwon Cho, and Jinsu Choi. Iris recognition using wavelet features. *Kluwer Academic Publishers, Journal of VLSI Signal Processing*, no. 38, pages 147–156, November 2004.
12. Shinyoung Lim, Kwanyong Lee, Okhwan Byeon, and Taiyun Kim. Efficient iris recognition through improvement of feature vector and classifier. *ETRI Journal*, vol. 23, no. 2, pages 61–70, June 2001.
13. Li Ma, Tieniu Tan, Yunhong Wang, and Dexin Zhang. Personal identification based on iris texture analysis. *IEEE Transactions on Pattern Analysis and Machine Intelligence*, vol. 25, no. 12, pages 1519–1533, December 2003.
14. Li Ma, Yunhong Wang, and Tieniu Tan. Iris recognition using circular symmetric filters. In *Proceedings of the 15th International Conference on Pattern Recognition (ICPR02)*, vol. 2, pages 414–417, 2002.
15. Li Ma, Yunhong Wang, and Dexin Zhang. Efficient iris recognition by characterizing key local variations. *IEEE Transactions on Image Processing*, vol. 13, no. 6, pages 739–750, June 2004.
16. D. Martin-Roche, C. Sanchez-Avila, and R. Sanchez-Reillo. Iris recognition for biometric identification using dyadic wavelet transform zero-crossing. *IEEE Aerospace and Electronic Systems Magazine*, Mag. 17, No. 10, pages 3–6, 2002.
17. Multimedia University. MMU iris image database, 2004. <http://pesona.mmu.edu.my/ccteo>
18. Hugo Proença and Luís A. Alexandre. UBIRIS: A noisy iris image database. In *13th International Conference on Image Analysis and Processing (ICIAP2005)*, pages 970–977, September 2005. <http://iris.di.ubi.pt>
19. Hugo Proença and Luís A. Alexandre. Iris segmentation methodology for non-cooperative iris recognition. *IEE Proc. Vision, Image & Signal Processing (To appear)*, 2006.
20. C. Sanchez-Avila and D. Martin-Roche. Iris-based biometric recognition using dyadic wavelet transform. *IEEE Aerospace and Electronic Systems Magazine*, pages 3–6, 2002.
21. University of Bath. University of Bath iris image database, 2004. [www.bath.ac.uk/elec-eng/pages/sipg/](http://www.bath.ac.uk/elec-eng/pages/sipg/)
22. Mayank Vatsa, Richa Singh, and A. Noore. Reducing the false rejection rate of iris recognition using textural and topological features. *International Journal of Signal processing*, vol. 2, no. 1, pages 66–72, 2005.

23. Richard P. Wildes. Iris recognition: an emerging biometric technology. In *Proceedings of the IEEE*, vol. 85, no.9, pages 1348–1363, U.S.A., September 1997.
24. Yong Zhu, Tieniu Tan, and Yunhong Wang. Biometric personal identification based on iris patterns. In *Proceedings of the 13th International Conference on Pattern Recognition (ICPR00)*, pages 2801–2804, 2000.